



# Influence of polyethylene cross-linked functionalization on the interfacial properties of carbon nanotube-reinforced polymer nanocomposites: a molecular dynamics study

S. Haghighi<sup>1</sup> · R. Ansari<sup>2</sup> · S. Ajori<sup>3</sup>

Received: 8 November 2018 / Accepted: 5 March 2019 / Published online: 29 March 2019  
© Springer-Verlag GmbH Germany, part of Springer Nature 2019

## Abstract

The average pull-out force and interaction energy of polyethylene (PE) cross-linked functionalized carbon nanotubes (cfCNTs) embedded in polymer matrices (PE-cfCNTs@polymers) was studied using molecular dynamics (MD) simulations. Accordingly, the pull-out process of PE-cfCNTs from inside polymer matrices, i.e., Aramid and PE, was performed under displacement control. The results obtained were compared with those of pure carbon nanotube (CNT) incorporated into polymer matrices (pure CNT@polymers). The influence on the pull-out force and interaction energy between the CNT and polymer of the structure of polymer matrices, the weight percentage and two types of distribution patterns of cross-linked PE chains, namely mapped and wrapped, was investigated. The results indicate that the structure of the polymers and distribution patterns of cross-linked PE chains strongly affect important parameters related to interfacial properties. The average pull-out force of mapped and wrapped PE-cfCNTs@polymers increases as the weight of attached PE chains on the CNT surface increases. The effect of wrapped structures on increasing the pull-out force is greater than that of the mapped configurations. Also, the PE-cfCNTs@polymers show higher average pull-out forces than those of their pure counterparts. As the CNT pulls out from the polymer matrix, an approximately linear reduction in the absolute value of interaction energy with the pull-out displacement is observed. However, this trend is changed to some extent by imposing instability through the wrapped PE-cfCNTs.

**Keywords** Carbon nanotube · Functionalization · Pull-out · Molecular dynamics simulations

## Introduction

The remarkable mechanical and physical properties of carbon nanotubes (CNTs), such as high strength, tensile modulus, and high aspect ratio, have made them ideal reinforcing agents in polymer nanocomposites [1–6]. Thus, great interest has been demonstrated in experimental [3, 7, 8] and theoretical [9, 10] studies to understand the mechanical and thermal properties of CNT/polymer nanocomposites, which are considered as a

new generation of lightweight and high-strength nanocomposites. Despite the superior properties mentioned above for the CNTs, very strong interactions between the walls of CNTs and, consequently, the high agglomeration tendency of CNTs to form ropes and stabilized bundles, restrict the uniform dispersion of CNTs within matrices, which leads to poor load transfer at interfaces [11, 12]. Moreover, the degree of interfacial adhesion between the CNT and the supporting matrix, which determines the efficiency of the transferability of load at the interphase region, is another challenging issue [13, 14]. To overcome these drawbacks, chemical modification processes such as covalent functionalization have been employed as one of the most effective strategies [15–18]. In covalent functionalization, the intrinsic physiochemical properties of the host nanostructure change through altering the sp<sup>2</sup> hybridization of CNTs and their surface polarity [19–21]. In this regard, the chemical approach has been used in the covalent functionalization of CNTs with functional groups like PE to improve both the interfacial adhesion of CNTs with polymers and the elastic properties of the resulting

✉ R. Ansari  
r\_ansari@guilan.ac.ir

<sup>1</sup> Department of Mechanical Engineering, University of Guilan, University Campus2, Rasht, Iran

<sup>2</sup> Department of Mechanical Engineering, University of Guilan, PO Box 3756, Rasht, Iran

<sup>3</sup> Department of Mechanical Engineering, University of Maragheh, Maragheh, East Azerbaijan Province, Iran

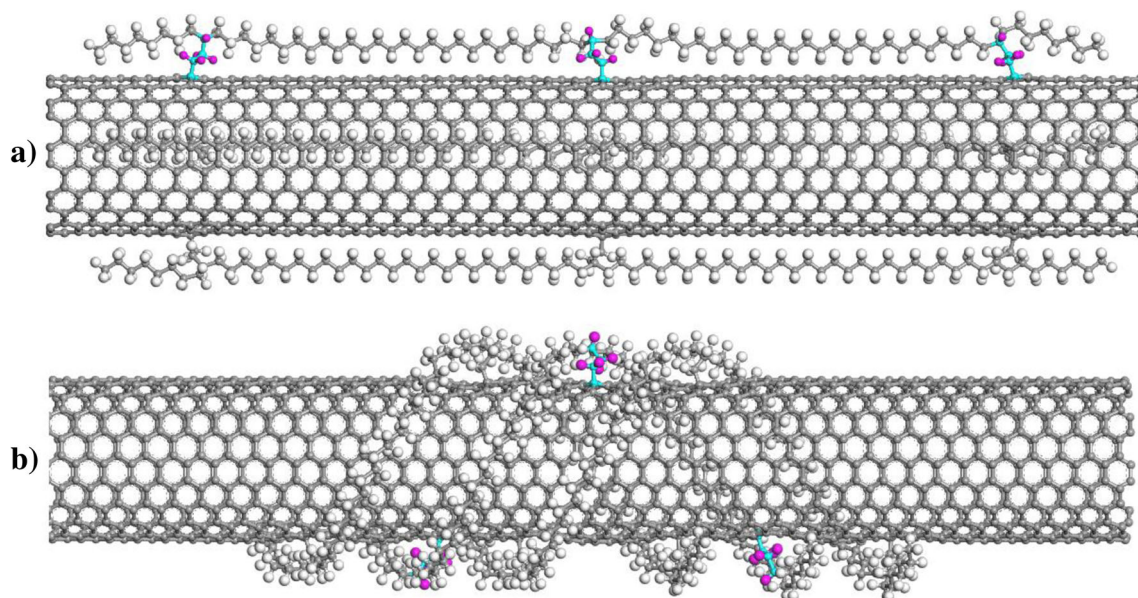


**Fig. 1** Schematic representation of **a** mapped polyethylene (PE) cross-linked functionalized carbon nanotube (PE-cfCNT), **b** wrapped PE-cfCNT

nanocomposites [1, 16, 22]. A review of the existing literature illustrates that a number of experimental, numerical and analytical studies have been conducted to investigate load transfer issues and interfacial behavior in CNT/polymer systems [23–28]. The interfacial and mechanical properties of two-phase nanocomposites, such as interfacial shear stress (ISS), tensile and fracture strength, were found to depend notably on the structure and characteristics of the interface [1, 29–32]. Furthermore, large discrepancy in experimental findings were observed owing to the difficulties of manipulation and evaluation of strain and force at nanoscale. To help address this issue, computational approaches like continuum mechanics, molecular dynamics (MD), molecular mechanics (MM), and a combination of MD and MM have received much attention. According to previous numerical simulations, the pull-out test of CNT in polymer matrices is an effective method with which to assess the interfacial properties of the CNT/polymer nanocomposites, e.g., interfacial bonding energy, which determines the load-carrying capacity from the supporting matrix

to the CNT [13, 33–36]. For instance, Chawla et al. [37] explored Young's modulus and ISS of CNT embedded in a PE matrix by employing MD simulation of a pull-out test. Their findings illustrated that increased strain affects Young's modulus of CNT. Also, the longitudinal Young's modulus of CNT reduced during the pull-out process. Among other studies in the realm of polymer nanocomposites, several research studies have been carried out to assess the reinforcement influence on the interfacial response for load transfer issues of the three-dimensional (3D) structures of graphene sheets/CNTs (Gr/CNTs) known as hybrid systems [18, 38]. In these studies, the processes of opening and sliding separation at the interface, and in the matrices throughout the pull-out test, were taken into consideration. The presence of hybrid Gr/CNT structures in nanocomposites led to improved mechanical and electrical properties of the supporting matrix and, ultimately, the performance of the system. Zheng et al. [22] investigated the influence on parameters pertaining to the interfacial properties of modifying the surface of CNT with various

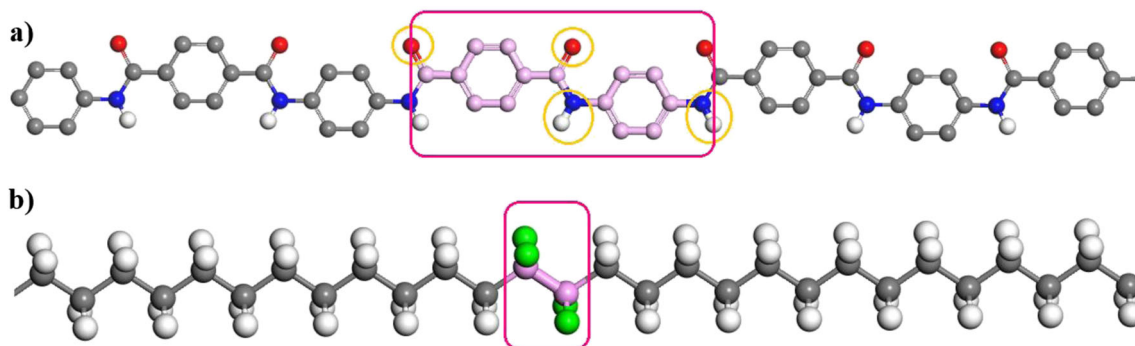


**Fig. 2a,b** Initial representation of non-covalent polymer chains. **a** Aramid, **b** PE. The repeating units are indicated in *pink* within an outlined *box*

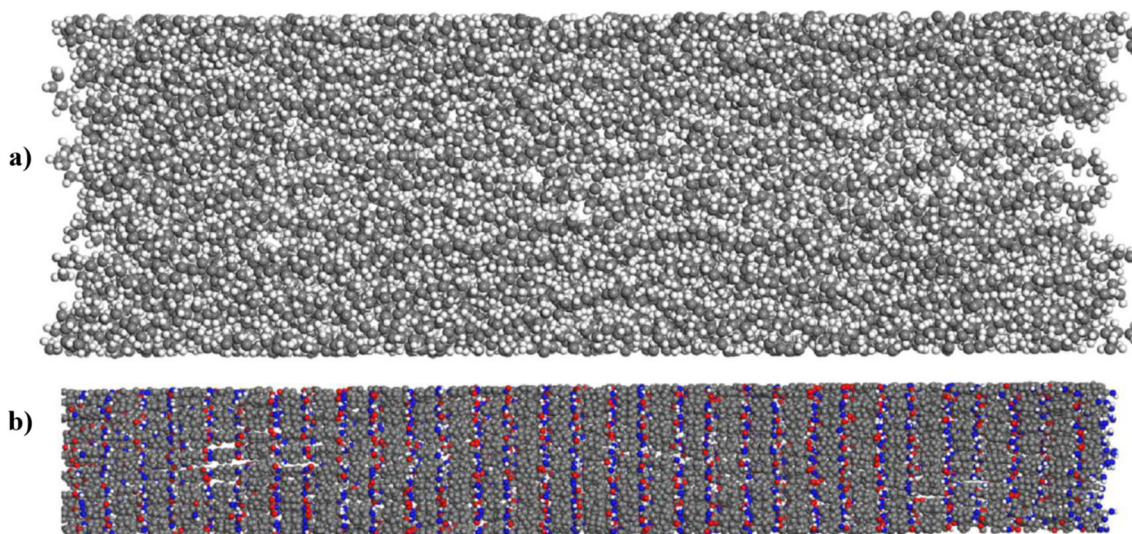


**Fig. 3** Schematic representation of **a** PE matrix, **b** Aramid matrix

functional groups. Their pull-out simulations reveal that the effective contact area between the functionalized CNT and the PE matrix increases drastically, leading to increased interfacial bonding between the constituent phases. It was also found that the structure of the functional groups is of great importance in determining adhesion to the polymer matrix. A literature review shows that, among MD-based studies, simulations of the pull-out process of functionalized carbon nanotubes (fCNTs) considering various polymer matrices for better understanding of the interfacial behavior of nanocomposites have received little attention. In particular, investigation of the effects of CNT functionalization in terms of the weight percentage and distribution pattern of functional groups has not yet been

performed. Hence, in the study reported herein, MD simulations of the pull-out process for PE-cfCNTs@polymers were performed to evaluate the influences on the average pull-out force and interaction energy of cross-linked functionalization of CNTs and different types of polymers as matrices.

## Methodology and models

### Methods

In the present study, the average pull-out force and interaction energy of PE-cfCNTs@polymers related to the interfacial

**Fig. 4** Variation in average pull-out force with displacement for (10, 10) CNT@PE at a CNT volume fraction of 9.5%

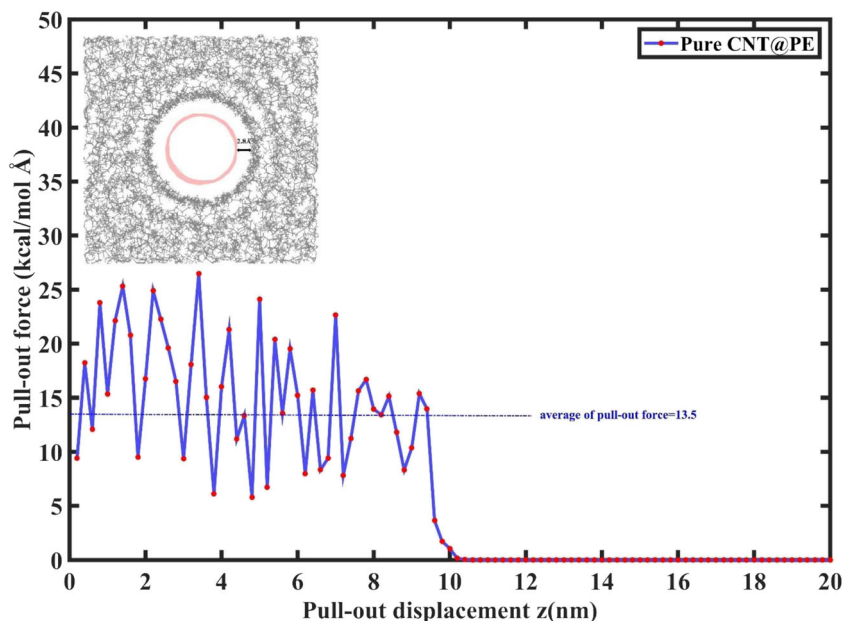
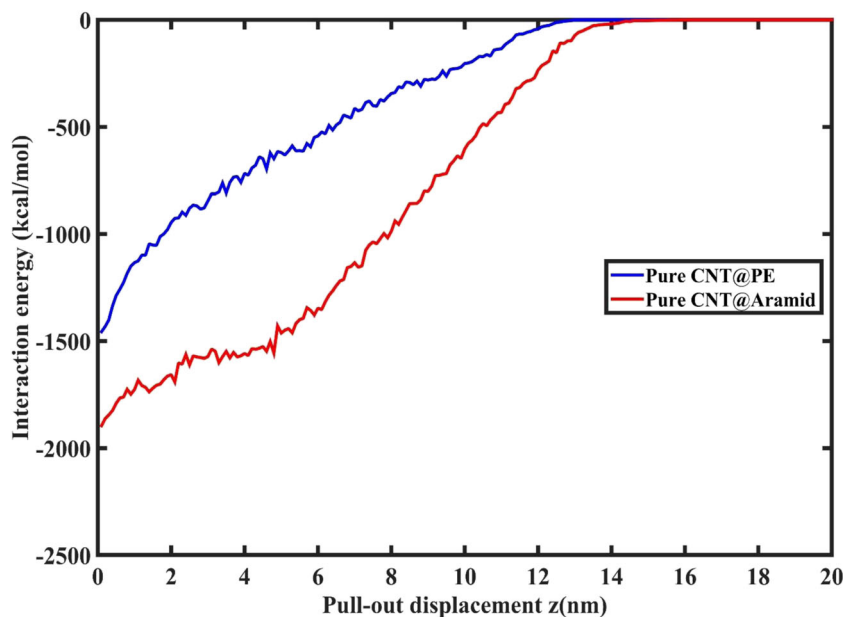


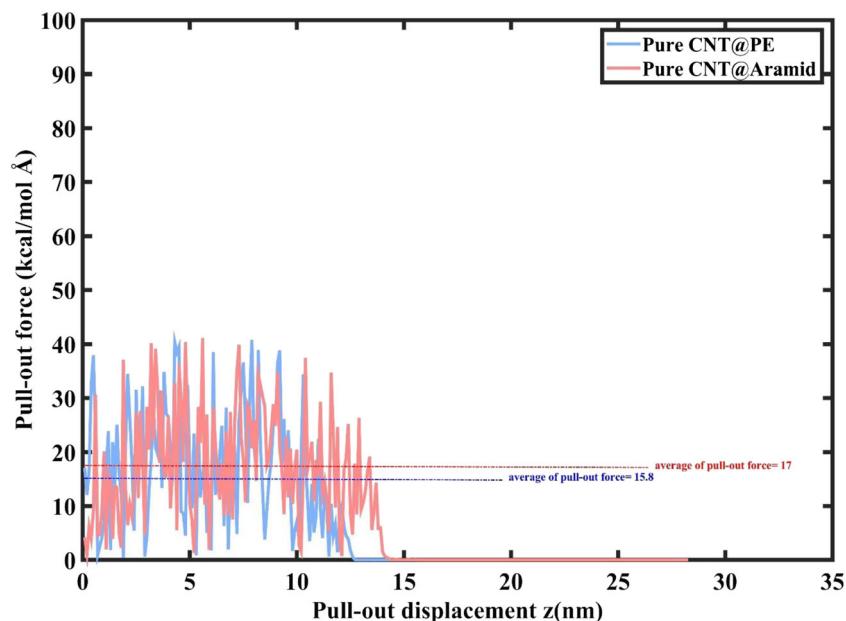
**Fig. 5** Variation in interaction energy with displacement for pure CNT@polymers



properties of generated nanocomposites were calculated by MD simulations conducted with the aid of the large-scale atomic/molecular massively parallel simulator (LAMMPS) [39]. A familiar force field in the molecular analysis of two-phase CNT/polymer nanocomposites, i.e., AMBER force field [40, 41], was chosen to model interatomic interactions between each pairs of atoms. Also, the classical Newtonian equations of motion of a large number of atoms, which assess a set of interacting atoms in time, were solved based on the Velocity-Verlet integrator algorithm together with the Nosé–Hoover thermostat algorithm. The use of these two algorithm

schemes with a time step of 0.5 fs not only ensures the stability of the system, but also leads to the reduction of temperature fluctuations [42, 43]. Firstly, to carry out the equilibration process at room temperature  $T = 300$  K, all models were minimized with regard to periodic boundary conditions for all directions of the MD simulation box. Afterwards, the systems are relaxed within the NVT canonical ensemble for 500 ps. Following this step, the systems were placed into the NPT isothermal-isobaric ensemble at the above-mentioned temperature and a pressure of  $P = 10$  atm for a further 1 ns. The models were then put into the NVT at  $T = 300$  K for another

**Fig. 6** Variation in average pull-out force with displacement for pure CNT@polymers



500 ps to attain their equilibrium state of structure and energy. In a subsequent step, a simulation of a pull-out test along the axial direction of the CNT (z-axis) was performed by applying a displacement of 1 Å to the clamped boundary of the fully embedded CNT (displacement-controlled load method). Note that, in the clamped boundary conditions, four rows of atoms are held fixed. It should be mentioned that, as the CNTs pull out from the polymers, the boundary conditions in the *x*- and *y*-directions are also kept periodic.

### Details of selected potential function (AMBER force field) in MD simulation

The Amber force field was designed as a successor to Weiner's force field [44] to describe intermolecular interactions, e.g., Lennard–Jones (LJ) and Coulombic, and to model conformational energies in a molecular system. As all interactions in molecules containing C, H, O, N, S, P and halogens can be modeled by the Amber force field, it is widely used in atomistic simulations of nucleic acids, proteins and other organic molecules in biological chemistry. A general version of the AMBER force field for every particular system is composed of a formula part that defines it in terms of different energies, and a coefficients part that is assigned to entire bonds and atoms. The energy expressions applied in the Amber force field are given in the following equation:

$$E_{\text{potential}} = E_{\text{bonds}} + E_{\text{angles}} + E_{\text{dihedrals}} + E_{\text{coulombic}} + E_{\text{vdWaal}} \quad (1)$$

The terms  $E_{\text{bonds}}$ ,  $E_{\text{angles}}$ ,  $E_{\text{dihedrals}}$ ,  $E_{\text{coulombic}}$  and  $E_{\text{vdWaal}}$  refer to bonds, angles, dihedrals, Coulombic and van der Waals (vdW) interaction potentials, respectively, which are obtained by:

$$E_{\text{bonds}} = \sum_{\text{bonds}} k_r (r - r_{\text{eq}})^2 \quad (2)$$

$$E_{\text{angles}} = \sum_{\text{angles}} k_{\theta} (\theta - \theta_{\text{eq}})^2 \quad (3)$$

$$E_{\text{dihedrals}} = \frac{V_n}{2} [1 + \cos(n\varphi - \gamma)] \quad (4)$$

$$E_{\text{coulombic}} = \sum_{i < j} \left[ \frac{q_i q_j}{\epsilon R_{ij}} \right] \quad (5)$$

$$E_{\text{vdWaal}} = \sum_{i < j} \left[ \frac{A_{ij}}{R_{ij}^{12}} - \frac{B_{ij}}{R_{ij}^6} \right] \quad (6)$$

where the values of the required parameters in their formulas were determined accurately by Cornell et al. [41]. The first three terms in the interatomic potential are related to the bonded interactions, and vdW interaction potential together with Coulombic evaluate non-bonded interactions such as electrostatic interactions. It

is worth noting that in Eq. (6), LJ pair potential is used to define vdW interactions.

### Simulation models

Herein, a (10, 10) armchair CNT with a length of ~100 Å, which includes 1640 atoms, was chosen. To functionalize the CNT, up to four PE chains were bonded to the surface of the CNT in either a mapped or wrapped distribution pattern. Also, the weight percentage of covalently attached PE chains varies from ~6% to 24%. Note that, in the current study, 1cfCNT, 2cfCNT, 3cfCNT and 4cfCNT refer to CNT functionalized by one to four PE chains, respectively. As it can be illustrated in Fig. 1, the difference between the two structures is related to the attachment configuration of PE chains on CNTs. In the mapped configuration, the PE chain is linked at three points along the CNTs axis, whereas a helical wrapping attachment of PE chain around the CNT is performed in the wrapped distribution pattern.

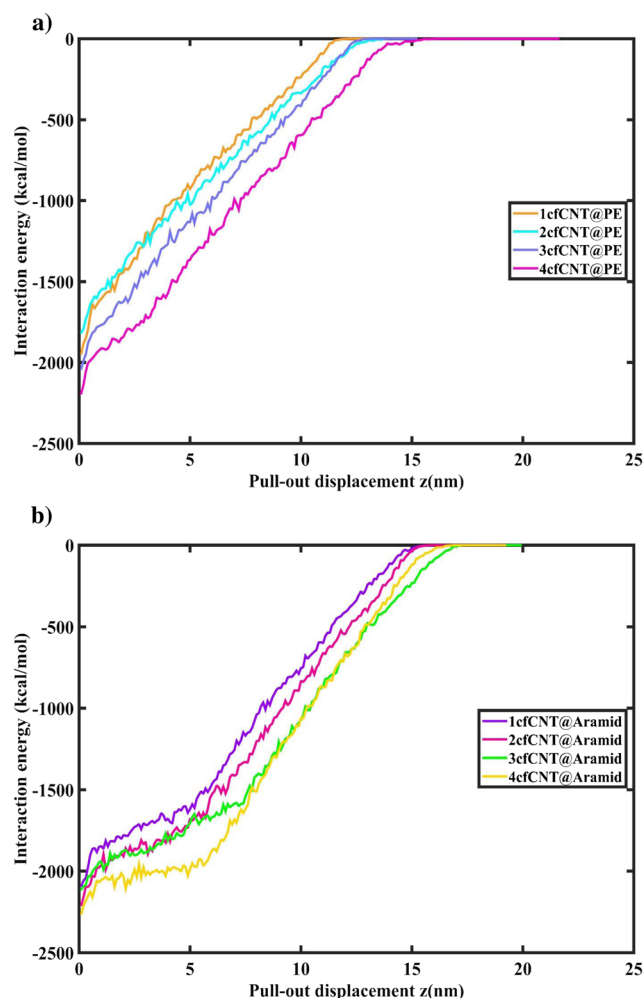
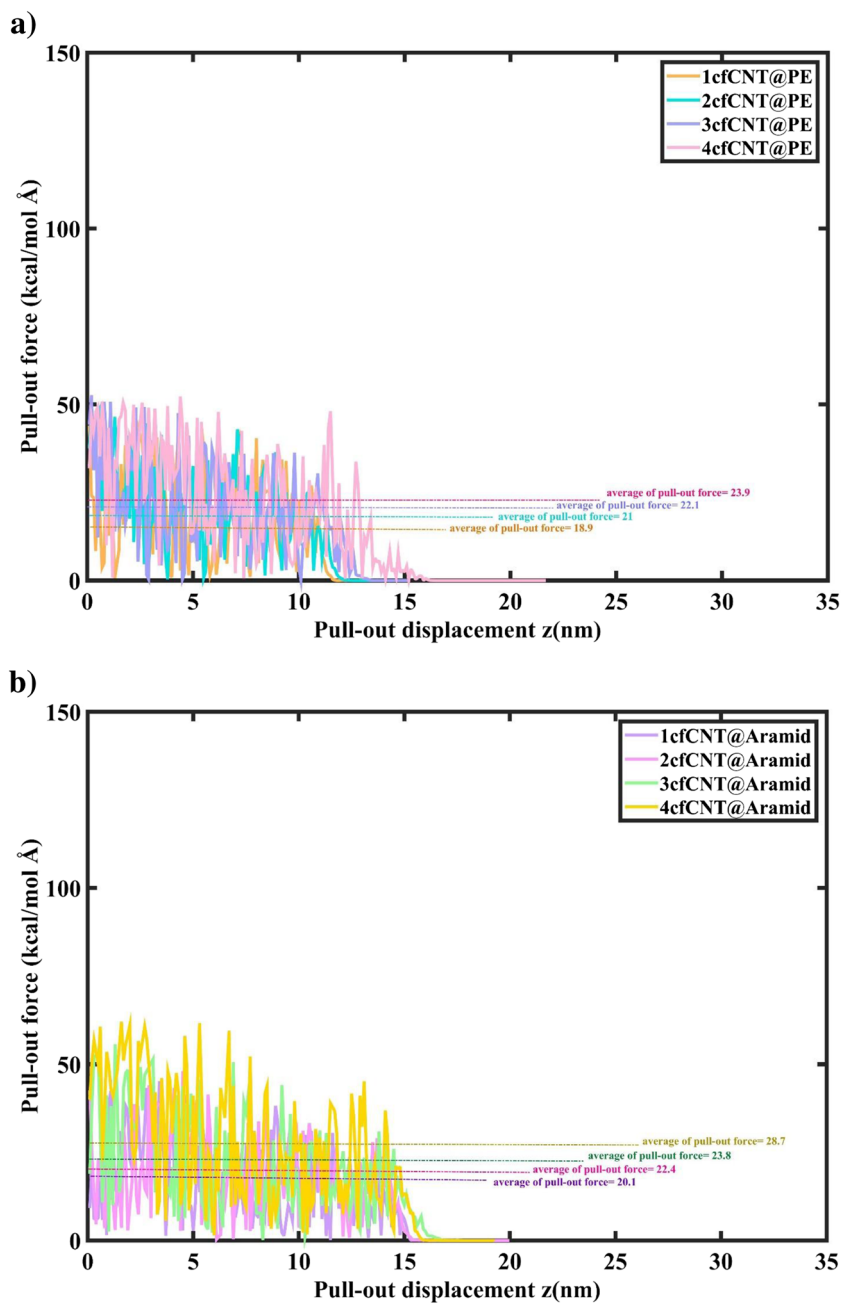


**Fig. 7a,b** Variation in interaction energy with displacement for mapped configurations. **a** PE-cfCNT@PE, **b** PE-cfCNT@Aramid

To investigate the effect of polymer structure on interfacial properties, two types of polymers, namely PE and Aramid (a commonly used composite material in aerospace and military industries with a relatively rigid backbone) as matrices, were modeled. Thanks to the simplicity of hydrocarbon configurations and their widespread applications in various engineering fields, the PE molecule [16, 34, 45], i.e.,  $(C_2H_4)_n$ , was selected to fabricate polymer chains with flexible backbones. Therefore, a PE matrix of 48 chains with 60 repeating units in each chain was simulated. By embedding a pure CNT almost at the center of the prepared PE matrix, the dimensions of the equilibrated system obtained were around

$39\text{\AA} \times 39\text{\AA} \times 128\text{\AA}$ . Moreover, Aramid [46, 47],  $(-CO-C_6H_4-CO-NH-C_6H_4-NH-)_n$ , was used to construct a matrix that includes 52 chains with 16 repeating units in each chain. In this case, the equilibrated system is composed of a rectangular box with the dimensions of  $49\text{\AA} \times 28\text{\AA} \times 204\text{\AA}$ . A sample of polymer chains is illustrated schematically in Fig. 2. It should be noted that, since the density of matrix and volume fraction of CNT are of extreme significance in determining the properties of nanocomposites, these variables in both pure CNT@polymers and PE-cfCNTs@polymers are considered almost close to each other. Accordingly, the average density of the equilibrated matrices and the CNT volume fraction in

**Fig. 8a,b** Variation in average pull-out force with displacement for mapped configurations. **a** PE-cfCNT@PE, **b** PE-cfCNT@Aramid



pure CNT@polymers were obtained as  $\sim 0.8 \text{ g cm}^{-3}$  and  $\sim 15\%$ , respectively. Further, the average value of the interfacial thickness in equilibrated systems was calculated at  $\sim 3.1 \text{ \AA}$ , which is in good agreement with the separation distance between a CNT and polymers used by Xiong and Meguid [27]. The initial schematic of polymer matrices is presented in Fig. 3.

## Results and discussion

### Model validation

To begin with, the average pull-out force of a (10, 10) CNT with a length of  $\sim 100 \text{ \AA}$  embedded in the PE matrix, which also has a volume fraction of 9.5%, was estimated. From this simulation, the equilibrated matrix density and thickness of interface between the CNT and the surrounding PE matrix were computed at about  $\sim 0.7 \text{ g cm}^{-3}$  and  $2.8 \text{ \AA}$ , respectively. Further, the axial displacement of the CNT at each step of the pull-out process was selected as  $2 \text{ \AA}$  to validate our results compared with those from an earlier MD-based investigation [34]. As can be observed in Fig. 4, the average pull-out force was obtained as  $\sim 13.5 \text{ kcal mol}^{-1} \text{ \AA}^{-1}$ , which is in good agreement with the value of  $\sim 15 \text{ kcal mol}^{-1} \text{ \AA}^{-1}$  calculated by Li et al. [34].

### Effect of polymer matrix structure on the interfacial properties of pure CNT@polymers

At the beginning, to study the influence of polymer structure on parameters affecting interfacial properties of nanocomposites, pure CNT@Aramid and CNT@PE were simulated; the results are shown in Figs. 5 and 6. The interaction energy changes almost linearly upon increasing displacement during the pull-out process, and vanishes after the CNT is completely moved away from the polymers (see Fig. 5). This occurs because of the reduction in effective interaction area during the process, and due to the stable interfacial binding interaction between the CNT and surrounding polymers. Moreover, as can be seen from Fig. 5, in every pull-out displacement the CNT and the Aramid attract each other with higher absolute values of attractive forces compared with CNT and PE. For example, at a displacement of 8 nm, the absolute value of interaction energy of pure CNT@Aramid is  $987.2 \text{ kcal mol}^{-1}$ , which is around 3 times higher than that of pure CNT@PE. The fact is that, compared with the hydrocarbon backbones in PE chains, the aromatic rings in Aramid chains provide a more effective interaction area with the CNT, which leads to increased number of vdW interactions in the interfacial region and, therefore, larger absolute values

of interaction energy. Furthermore, the results indicate that, after some fluctuations in the pull-out force, it gradually reduces to a value of zero where there is no vdW interaction between the CNT and polymers (see Fig. 6). Also, pure CNT@Aramid is found to possess higher average pull-out force compared to pure CNT@PE. As a result, the interfacial properties of nanocomposites fabricated using pure CNT@Aramid are better than those of pure CNT@PE.

### Effects of PE cross-linked functionalization of CNT and polymer matrix structure in PE-cfCNTs@polymers

This section focuses on the average pull-out force and interaction energy of PE-cfCNTs@polymers in comparison with those of pure CNT@polymers. By performing further simulations (Figs. 7, 8, 9 and 10), the influence of CNT functionalization is discussed in terms of the weight percentage of cross-linked PE chains as well as their configurations, i.e., mapped or wrapped.

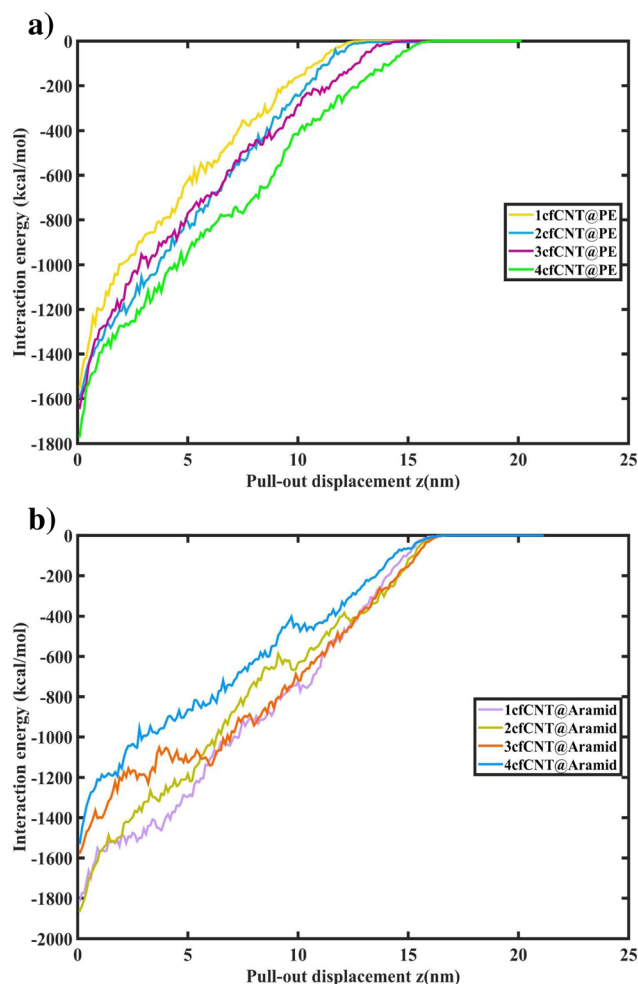
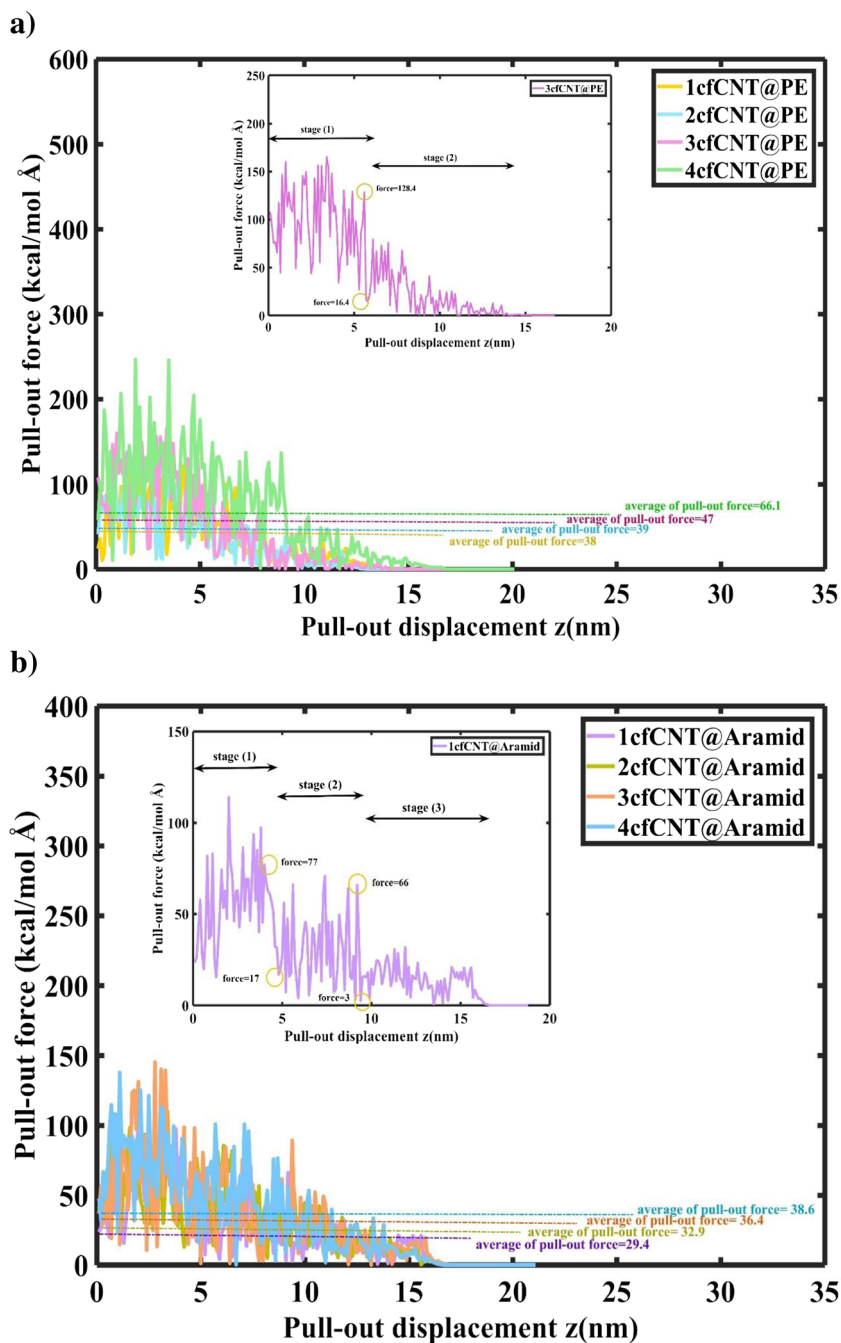


**Fig. 9a,b** Variation in interaction energy with displacement for wrapped configurations. **a** PE-cfCNT@PE, **b** PE-cfCNT@Aramid

**Fig. 10a,b** Variation in average pull-out force with displacement for wrapped configurations. **a** PE-cfCNT@PE, **b** PE-cfCNT@Aramid



### Mapped distribution pattern

Considering the functionalized CNTs with mapped distribution pattern, Figs. 7 and 8 illustrate the variation in interaction energy and pull out force with pull-out displacement for the both PE and Aramid polymer matrices. Based on the results from Fig. 7, which are similar to those of pure CNT@polymers, as the PE-cfCNTs pull away from matrices, the interaction energy decreases and then lies on the value of zero. Moreover, in every pull-out displacement, by increasing

the weight percentage of cross-linked PE chains, the interaction energy of mapped PE-cfCNTs@polymers generally increases, which means that, the more mapped PE cross-linked functional groups exist, the higher the number of vdW interactions between the CNT and surrounding matrix in the interface area. This results in an improvement in load transfer capability in the system (see Fig. 7). For instance, at a displacement of 6 nm, the absolute value of energy for the 4cfCNT@PE ( $1210 \text{ kcal mol}^{-1}$ ) is around 36%, 29% and 19% more than that of the 1cfCNT@PE ( $769.7 \text{ kcal mol}^{-1}$ ),

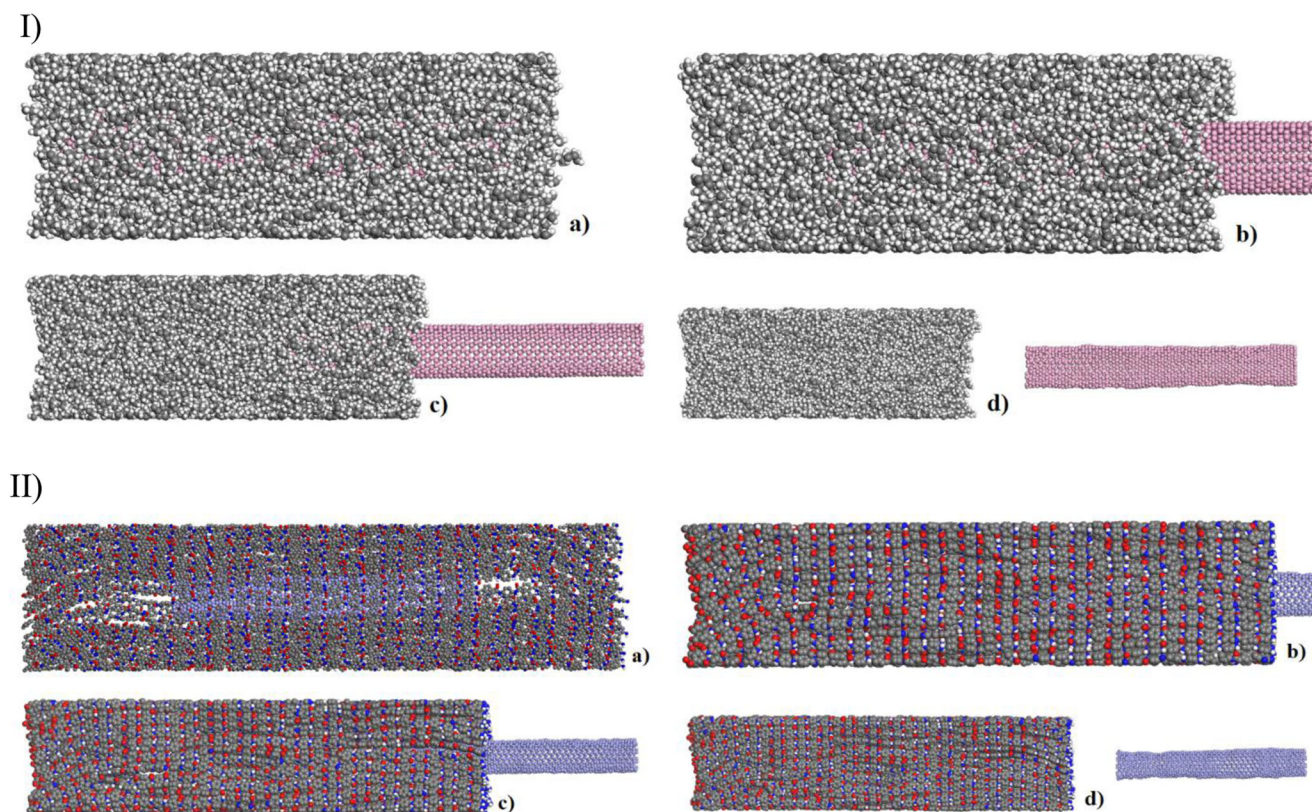


2cfCNT@PE ( $862.6 \text{ kcal mol}^{-1}$ ), and 3cfCNT@PE ( $975.1 \text{ kcal mol}^{-1}$ ), respectively (see Fig. 7a). According to the results, the mapped PE-cfCNTs@PE show higher interaction energies than pure CNT@PE, which can be attributed to the increase in surface roughness and the stronger interlocking of PE-cfCNT with its surrounding polymer chains compared to pure CNT. For example, at a displacement of 4 nm, there are the increases of about 30%, 36%, 43% and 54% in the interaction energy of 1cfCNT@PE, 2cfCNT@PE, 3cfCNT@PE, and 4cfCNT@PE compared to pure CNT@PE, respectively (see Figs. 5 and 7a). In addition, changing the type of polymer material from PE to Aramid shows that the absolute values of interaction energies in the mapped PE-cfCNTs@Aramid are considerably more than those of the mapped PE-cfCNTs@PE (see Fig. 7). This result is attributed to the relatively rigid backbone of Aramid, whose structure contains benzene rings and atoms with great reactivity, i.e., oxygen and nitrogen. As a consequence, not only can Aramid chains provide more effective interaction area with the mapped PE-cfCNT in the interfacial region, leading to a higher number of vdW interactions, they also have stronger binding interactions with the PE-cfCNT. Similarly, the results obtained for mapped PE-cfCNTs@Aramid compared to their pure counterparts illustrate that mapped PE-cfCNTs@Aramid has higher interaction energies than pure CNT@Aramid at the same displacement (see Figs. 5 and 7b). Furthermore, Fig. 8 clearly demonstrates

that the average pull-out force of PE-cfCNTs@polymers increases as the weight percentage of cross-linked PE chains increases. This means that the increased weight of attached PE chains results in enhanced interfacial resistance of the system. Also, it can be seen from Fig. 8 that, at every weight of attached PE chain, the mapped PE-cfCNT@Aramid can provide larger values of average pull-out forces in comparison with the mapped PE-cfCNT@PE. It can be noted from Figs. 6 and 8 that the average pull-out force of mapped PE-cfCNTs@polymers is higher than that of pure CNT@polymers, which implies considerable improvement in the interfacial resistance of mapped PE-cfCNTs@polymers compared to pure CNT@polymers. For example, the average pull-out force of 4cfCNT@PE and 4cfCNT@Aramid in the mapped distribution pattern is approximately 34% and 41% more than that of their corresponding pure CNT@polymers, respectively.

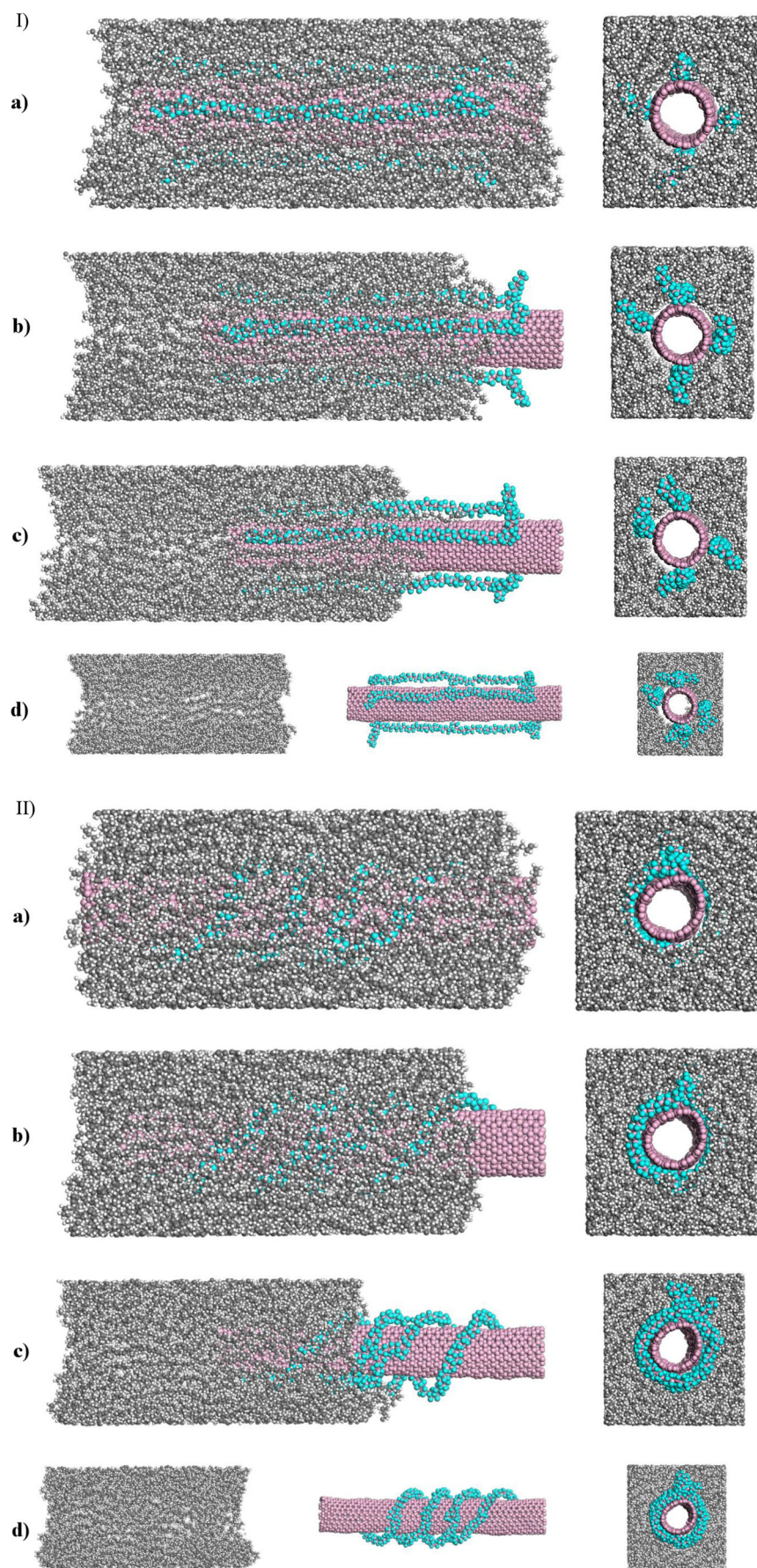
### Wrapped distribution pattern

The results of our thorough simulations corresponding to the wrapped distribution pattern can be seen in Figs. 9 and 10. As it can be seen from Fig. 9a, wrapped PE-cfCNTs tend to disturb the stability of the system, especially at a high weight percentage of cross-linked PE chains, i.e., 4cfCNT, leading to almost nonlinear changes in interaction energy during the



**Fig. 11** Examples of pullout simulations for **a** pure CNT@PE, **b** pure CNT@Aramid

**Fig. 12** Examples of pullout simulations for **a** mapped PE-cfCNT@PE, **b** wrapped PE-cfCNT@PE, **c** mapped PE-cfCNT@Aramid, **d** wrapped PE-cfCNT@Aramid



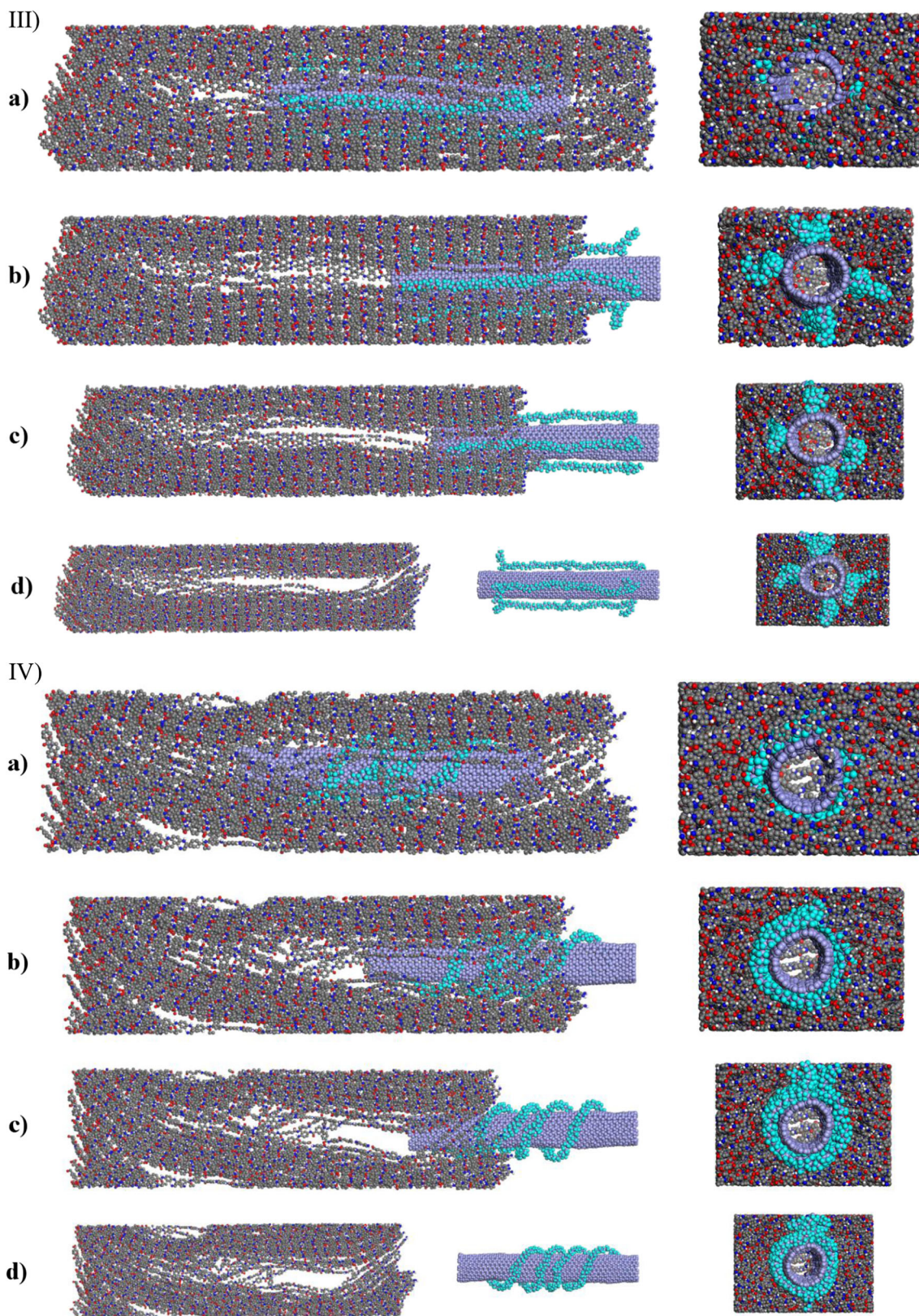


Fig. 12 continued.

pull-out process. Further, at every imposed displacement, the interaction energy of the wrapped PE-cfCNTs@PE increases

by increasing the weight of the cross-linked PE chain. Comparing Fig. 5 with Fig. 9a, it is found that, in terms of

specific displacement, wrapped PE-cfCNTs@PE possess larger absolute values of interaction energies than pure CNTs@PE. As a matter of fact, wrapped PE-cfCNTs can increase interlocking with the polymer chains and the number of vdW interactions within the interface area of PE-cfCNTs@PE compared to pure CNT@PE. Figure 9b implies that wrapped PE-cfCNTs drastically change the stability of the interface area. The fact is that the state of the cross-linked PE chain in the wrapped pattern causes non-uniform dispersal of Aramid chains around the CNT during the whole process, which results in a much lower effective interaction area within the interfacial region and, consequently, a substantial reduction in the absolute value of interaction energy compared with pure CNTs@Aramid (see Figs. 5 and 9b). In specific displacement, in general, wrapped PE-cfCNTs@Aramid has higher absolute values of interaction energies than wrapped PE-cfCNTs@PE. Figures 10a and b considering the average pull-out force in wrapped PE-cfCNTs@polymers. As can be seen in Fig. 10a, the variation trend in the pull-out force with displacement shows that there are two distinguishable phases as the wrapped PE-cfCNTs pull out from the PE matrix. At first, the pull-out force oscillates severely around a fixed range, then suddenly drops to a far low value; in the second phase, the force fluctuates gradually, reducing to a value of zero. These calculations illustrate that, by increasing the weight of wrapped PE chains, variations in energy in the system increase, which leads to drastic oscillations and obvious higher pull-out force in the first stage. The total average pull-out force of wrapped PE-cfCNTs@PE, including the forces in the first and second stages, illustrate that the effect of the wrapped configuration on increasing the pull-out force is more pronounced than in mapped and pure configurations. In wrapped PE-cfCNTs@Aramid (see Fig. 10b), the variation in pull-out force with displacement is divided into three phases. In the first and second stages, drastic fluctuations in the pull-out force can be seen, with each stage occurring around a certain range, and, after some small oscillations, the pull-out force reaches a value of zero. This behavior suggests that the wrapped structures exert their influence by disturbing the uniform distribution of Aramid chains with stiffer backbones and, therefore, the increase in the fluctuations of energy in the system during the whole process is greater than with PE chains. Consequently, the interfacial resistance is reduced; hence, the average pull-out forces of wrapped PE-cfCNTs@Aramid are lower than those of wrapped PE-cfCNTs@PE.

Finally, in order to further understand the pull-out process, some snapshots from pull-out test in the pure CNT and PE-cfCNTs@polymers are presented in Figs. 11 and 12.

## Conclusions

The main focus of the present study was to investigate the influence of cross-linked functionalization of the CNTs on two important parameters related to the interfacial properties of nanocomposites, i.e., pull-out force and interaction energy, through MD simulations. Based on the results, as pull-out displacement increases, the absolute value of interaction energy is reduced, finally reaching zero. However, unstable interfacial binding interactions in the wrapped systems, especially in PE-cfCNTs@Aramid led to nonlinear changes in the trend of interaction energy with pull-out displacement. The average pull-out forces obtained in both mapped and wrapped PE-cfCNTs@polymers were higher than those of the corresponding pure polymers. Further, by increasing the weight of cross-linked PE chains, the average pull-out force of the mapped and wrapped PE-cfCNTs@polymers increased and the wrapped configurations had considerable effect on increasing the pull-out force compared to the mapped ones. It is worth noting that incorporating the mapped cfCNTs inside an Aramid matrix with stiff backbones resulted in greater improvement in the interfacial properties than those obtained with mapped PE-cfCNTs@PE. By contrast, the influence on increasing of the pull-out force of wrapped cfCNTs embedded in the PE matrix with flexible backbones was more pronounced than with wrapped PE-cfCNTs@Aramid.

## References

- Gou J, Minaie B, Wang B, Liang Z, Zhang C (2004) *Comput Mater Sci* 31(3–4):225–236
- Hernandez E, Goze C, Bernier P, Rubio A (1998) *Phys Rev Lett* 80(20):4502
- Schadler LS, Giannaris SA, Ajayan PM (1998) *Appl Phys Lett* 73(26):3842–3844
- Hone J, Whitney M, Piskoti C, Zettl A (1999) *Phys Rev B* 59(4):R2514
- Rahmat M, Hubert P (2011) *Compos Sci Technol* 72(1):72–84
- Meguid SA, Al Jahwari F (2014) *Acta Mech* 225(4–5):1267–1275
- Qian D, Dickey EC, Andrews R, Rantell T (2000) *Appl Phys Lett* 76(20):2868–2870
- Barber AH, Cohen SR, Wagner HD (2003) *Appl Phys Lett* 82(23):4140–4142
- Bhuiyan MA, Pucha RV, Worthy J, Karevan M, Kalaitzidou K (2013) *Compos Struct* 95:80–87
- Liu YJ, Chen XL (2003) *Mech Mater* 35(1–2):69–81
- Ansari R, Ajori S, Rouhi S (2015) *Superlattice Microsc* 77:54–63
- Thostenson ET, Chou TW (2002) *J Phys D Appl Phys* 35(16):L77
- Al-Ostaz A, Pal G, Mantena PR, Cheng A (2008) *J Mater Sci* 43(1):164–173
- Mohammadpour E, Awang M, Kakooei S, Akil HM (2014) *Mater Des* 58:36–42
- Balasubramanian K, Burghard M (2005) *Small* 1(2):180–192
- Frankland SJ, Caglar A, Brenner DW, Griebel M (2002) *J Phys Chem B* 106(12):3046–3048

17. Zheng Q, Xue Q, Yan K, Gao X, Li Q, Hao L (2008) *Polymer* 49(3):800–808
18. Liu F, Hu N, Ning H, Atobe S, Yan C, Liu Y, Wu L, Liu X, Fu S, Xu C, Li Y (2017) *Carbon* 115:694–700
19. Ansari R, Ajori S, Rouhi S (2015) *Appl Surf Sci* 332:640–647
20. Ajori S, Ansari R, Darvizeh M (2015) *Phys B Condens Matter* 462: 8–14
21. Boroushakh SH, Ansari R, Ajori S (2018) *Diam Relat Mater* 86:173–178
22. Zheng Q, Xia D, Xue Q, Yan K, Gao X, Li Q (2009) *Appl Surf Sci* 255(6):3534–3543
23. Wagner HD, Lourie O, Feldman Y, Tenne R (1998) *Appl Phys Lett* 72(2):188–190
24. Cooper CA, Cohen SR, Barber AH, Wagner HD (2002) *Appl Phys Lett* 81(20):3873–3875
25. Lordi V, Yao N (2000) *J Mater Res* 15(12):2770–2779
26. Ang KK, Ahmed KS (2013) *Compos Part B* 50:7–14
27. Xiong QL, Meguid SA (2015) *Eur Polym J* 69:1–5
28. Wernik JM, Cornwell-Mott BJ, Meguid SA (2012) *Int J Solids Struct* 49(13):1852–1863
29. Meguid SA, Wernik JM, Cheng ZQ (2010) *Int J Solids Struct* 47(13):1723–1736
30. Koval'chuk AA, Shevchenko VG, Shchegolikhin AN, Nedorezova PM, Klyamkina AN, Aladyshev AM (2008) *Macromolecules* 41(20):7536–7542
31. Wernik JM, Meguid SA (2014) *Int J Solids Struct* 51(14):2575–2589
32. Han Y, Elliott J (2007) *Comput Mater Sci* 39(2):315–323
33. Chowdhury SC, Okabe T (2007) *Compos A Appl Sci Manuf* 38(3): 747–754
34. Li Y, Liu Y, Peng X, Yan C, Liu S, Hu N (2011) *Comput Mater Sci* 50(6):1854–1860
35. Frankland SJ, Harik VM (2002) Analysis of carbon nanotube pull-out from a polymer matrix. *MRS Online Proceedings Library Archive* 733
36. Liao K, Li S (2001) *Appl Phys Lett* 79(25):4225–4227
37. Chawla R, Sharma S (2017) Molecular dynamics simulation of carbon nanotube pull-out from polyethylene matrix. *Compos Sci Technol* 144:169–177
38. Im H, Kim J (2012) Thermal conductivity of a graphene oxide–carbon nanotube hybrid/epoxy composite. *Carbon* 50(15):5429–5440
39. Plimpton S (1995) *J Comput Phys* 117(1):1–9
40. Grindon C, Harris S, Evans T, Novik K, Coveney P, Laughton C (2004) Large-scale molecular dynamics simulation of DNA: implementation and validation of the AMBER98 force field in LAMMPS. *Philos Trans R Soc London A Math Phys Eng Sci* 362(1820):1373–1386
41. Cornell WD, Cieplak P, Bayly CI, Gould IR, Merz KM, Ferguson DM, Spellmeyer DC, Fox T, Caldwell JW, Kollman PA (1995) *J Am Chem Soc* 117(19):5179–5197
42. Ajori S, Ansari R, Darvizeh M (2016) *J Mol Model* 22(3):62
43. Hoover WG (1985) *Phys Rev A* 31(3):1695
44. Weiner SJ, Kollman PA, Case DA, Singh UC, Ghio C, Alagona G, Profeta S, Weiner P (1984) A new force field for molecular mechanical simulation of nucleic acids and proteins. *J Am Chem Soc* 106(3):765–784
45. Lv C, Xue Q, Xia D, Ma M (2012) *Appl Surf Sci* 258(6):2077–2082
46. Cao K, Siepermann CP, Yang M, Waas AM, Kotov NA, Thouless MD, Arruda EM (2013) *Adv Funct Mater* 23(16):2072–2080
47. Hillermeier K (1984) *Text Res J* 54(9):575–580

**Publisher's note** Springer Nature remains neutral with regard to jurisdictional claims in published maps and institutional affiliations.